Intersubband absorption line broadening in semiconductor quantum wells: Nonparabolicity contribution

M. Załużny
Institute of Physics, M. Curie-Skłodowska University, 20-031 Lublin pl., M. Curie-Skłodowskiej 1, Poland
(Received 11 May 1989; revised manuscript received 8 August 1990)

The influence of the conduction-band nonparabolicity on the intersubband absorption line broadening in $GaAs/Al_xGa_{x-1}As$ quantum wells is discussed in the framework of an empirical two-band model. In contrast with earlier papers, the influence of the depolarization effect on the absorption line shape is taken into account. The obtained results indicate that the contribution to the line broadening resulting from the nonparabolicity is, to a large extent, compensated for by the depolarization effect.

The problem of the intersubband line broadening in $GaAs/Al_xGa_{1-x}As$ quantum wells (QW's) arising from the intrinsic (bulk) nonparabolicity of the well (W) and barrier (B) materials as well as from the difference of the effective masses in these materials is the subject of many recent theoretical investigations.[1-4] The authors concentrate mainly on a detailed calculation of the subband dispersion relation using multiband $\mathbf{k}\cdot\mathbf{p}$ models, with different degrees of sophistication, to present the bulk band structure of the constituent materials. Unfortunately, they completely neglect the influence of the depolarization effect on the width of the absorption line. The object of this paper is to show that the inclusion of this effect is essential in an accurate description of the absorption line shape when the conduction band of the bulk crystal is not parabolic.

Several schemes[5-10] have been proposed to take the nonparabolicity into account. For our purpose the most convenient is an empirical two-band model for the heterostructures.[9,10] Following Refs. 9 and 10 we assume that the bulk band structure of the well and barrier materials is described by the two-band $\mathbf{k}\cdot\mathbf{p}$ Hamiltonian in which $E_p=2m_0p^2/\hbar^2$ (p is the interband-momentum matrix element) and energy gap E_g are eliminated in favor of the electron effective mass m and nonparabolicity parameter γ using the following relations:

$$m_0/m=2E_p/(3E_g),\quad \gamma=\hbar^2/(2mE_g)\ . \tag{1}$$

The energy dispersion relations for the electrons in the well and barrier material resulting from this model can be written in the form

$$E(k_W,k_t)=(E_M/2)\{[1+(4/E_M)(\mathcal{E}_{Ml}+\mathcal{E}_{Mt})]^{1/2}-1\}+V_M\ , \tag{2}$$

where the subscript $M=B$ or W, $V_W=0$, $V_B=V$ is the barrier height at the interfaces, $\mathcal{E}_{Ml}=\hbar^2k_{Ml}^2/2m_M$, $\mathcal{E}_{Mt}=\hbar^2k_t^2/2m_M$, $m_{W(B)}$ is the band-edge effective mass of the $W(B)$ material, $E_W=\hbar^2/(2m_W\gamma_W)$ and $E_B=E_W(m_B/m_W)$ are the effective energy gaps of the W and B materials, respectively, and γ_W is the nonparabolicity parameter of the well material.[9] We should remember that in the empirical two-band model m_W, m_B, and γ_W are adjustable parameters. The wave-vector components along the normal to the layer plane (x,y) and transverse to it are denoted by k_{Ml} and k_t, respectively.

Solving the empirical two-band $\mathbf{k}\cdot\mathbf{p}$ Hamiltonian in the framework of the envelope function approximation (for details see Refs. 5 and 11) we find the following bound-state eigenvalue equation for allowed values of k_{Ml}:

$$[rk_{Wl}\tan(k_{Wl}L/2)-ik_{Bl}][rk_{Wl}\cot(k_{Wl}L/2)+ik_{Bl}]+[k_t(r-1)/2]^2=0\ , \tag{3}$$

where $r=m_B[1-(V-E)/E_B]/m_W[1+E/E_W]$ and L is the width of the well.

The subband dispersion relation $E_n(k_t)\equiv E(k_{Wl}^{(n)}(k_t),k_t)$ and difference $\Delta E_{n'n}(k_t)=E_{n'n}(0)-E_{n'n}(k_t)$ [where $E_{n'n}(k_t)=E_{n'}(k_t)-E_n(k_t)$], resulting from Eqs. (2) and (3), for $GaAs/Al_{0.35}Ga_{0.65}As$ QW's (with $L=75$ Å and 100 Å) are shown in Fig. 1. For comparison, results obtained in the parabolic approximation[2] ($\gamma_W=0$) are also shown. (In the numerical calculations parameters m_W, m_B, γ_W, and V have been taken the same as in Ref. 9.) In both models $\Delta E_{n'n}(k_t)$ increases nearly linearly with increasing k_t^2. However, in the two-band model, this increase is faster. The numerical calculations show that the ratio $R_{21}=[\Delta E_{21}(k_t)]_{\text{nonpar}}/[\Delta E_{21}(k_t)]_{\text{par}}$ changes from 2 to 5 within the thickness range 75–150 Å. This result is consistent with that obtained by Ikonić *et al.*[2,4] It is interesting to note that in the empirical two-band model, in contrast with the parabolic model, the dependence of k_{Wl} on k_t has a vanishingly small influence on the subband dispersion (see Fig. 1). Further, we neglect this dependence, i.e., we assume that $E_n(k_t)=E(k_{Wl}^{(n)}(0),k_t)$.

When an external electric field $Ee^{-i\omega t}$ is applied in the z direction the absorbing power of the QW of unit area is proportional to the real part of the zz component of the modified two-dimensional frequency-dependent conductivity tensor $[\tilde{\sigma}(\omega)]$. Since in the QW's considered here the nonparabolicity correction to the subband dispersion is small, $\tilde{\sigma}_{zz}(\omega)$ can be calculated in a way similar to that described in Ando's paper.[12] Assuming that $\hbar\omega$ is close

to the subband separation $E_{n1}=E_{n1}(0)$ and neglecting for simplicity the excitonlike effect we find

$$\mathrm{Re}\sigma_{zz}(\omega)=(2e^2N_s z_{n1}^2\omega/E_{n1})\mathrm{Im}\tilde{G}_{1n}(\omega)\ , \tag{4}$$

with

$$\tilde{G}_{1n}(\omega)=G_{1n}(\omega)[1+\alpha_{nn}G_{1n}(\omega)]^{-1}\ , \tag{5}$$

where

$$G_{1n}(\omega)=(1/2\pi^2N_s)\times\int d\mathbf{k}_t F_{1n}(k_t)\frac{E_{n1}^2}{E_{n1}^2(k_t)-(\hbar\omega)^2-i\hbar\omega\Gamma}\ , \tag{6}$$

and

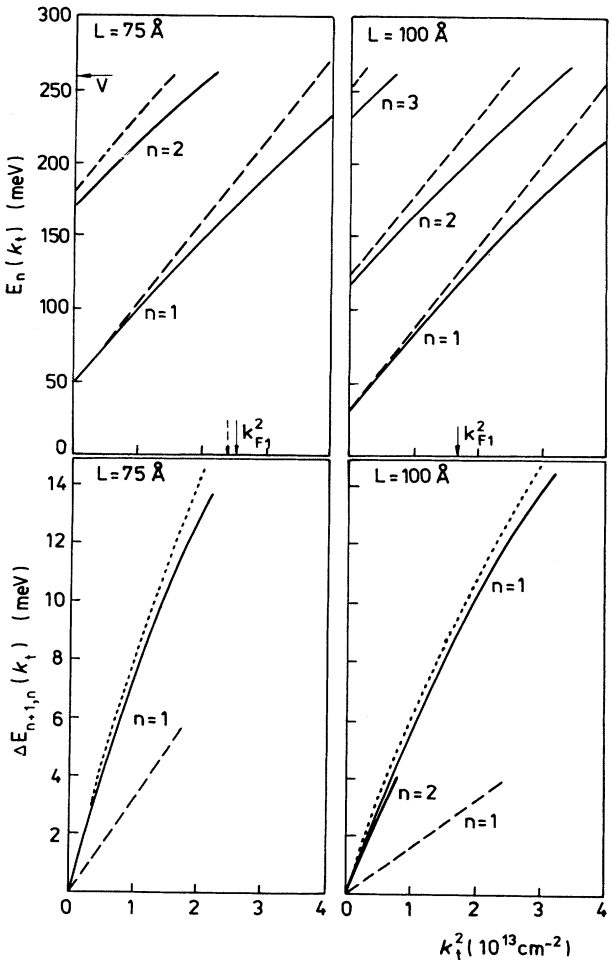

FIG. 1. Dependence of the electron energy and subband separation $\Delta E_{n+1,n}$ $(n=1,2)$ on k_t^2 in GaAs/$Al_{0.35}Ga_{0.65}$As QW's with $L=75$ and 100 Å. The solid lines contain intrinsic nonparabolicity of the bulk crystal, dashed lines do not. In the calculations only the states with the energy below the barrier height V are considered. For comparison we show also the results when nonparabolicity effects are taken into account but dependence of $k_{Wl}^{(n)}$ on k_t is ignored (dotted lines). The scale of the upper part of the figure is insufficient for distinguishing between the solid and dotted curves.

$$\alpha_{nn}=8\pi[N_s(1)-N_s(n)]e^2L_{nn}/E_{n1}\epsilon_\infty\ . \tag{7}$$

Here N_s is the surface density of the electrons, $N_s(n)$ is the surface density in subband n, $F_{1n}(k_t)=f_{\mathrm{FD}}(E_1(k_t))-f_{\mathrm{FD}}(E_n(k_t))$ is the difference of the Fermi-Dirac distribution functions calculated at $E_1(k_t)$ and $E_n(k_t)$, Γ is the phenomenological parameter describing the line broadening induced by the electron scattering, and ϵ_∞ is the dielectric constant. The parameter L_{nn} is defined in the same way as in Ref. 13. [Deriving Eq. (4) we have used the two-subband approximation[12,14] and neglected the change of the matrix element z_{n1} with k_t.]

The Fermi energy E_F appearing in the Fermi-Dirac distribution function can be obtained from the normalization condition $2\sum_{nk_t}f_{\mathrm{FD}}(E_n(k_t))=N_s$. At low temperature, when electron gas is strongly degenerated $(\nu=\hbar^2\pi N_s/m_W k_B T>3)$, E_F may be approximated by the formula $E_F=E_1(k_F)$ where $k_F=(2\pi N_s)^{1/2}$ is the Fermi wave vector. [We assume that only the ground subband $n=1$ is occupied, i.e., $k_F<k_{F1}$, where k_{F1} is the solution of $E_1(k_t)=E_2(0)$.] Calculation of E_F for higher temperature is a more difficult task. Fortunately, in the GaAs/Al_xGa_{1-x}As QW's where subband resonances have been observed (i) subband separation E_{21} is larger than the thermal energy k_BT, (ii) the nonparabolicity of the ground subband is not strong. Thus, for our purposes it will be sufficient to calculate E_F (when $\nu>3$) treating the carriers in the QW as a pure two-dimensional electron gas with effective mass $m^*=m_W$. Then $E_F=E_1(0)+k_BT\ln[\exp(\hbar^2k_F^2/2m_Wk_BT)-1]$.

The absorption line profile is essentially determined by the behavior of the function $\mathrm{Im}\tilde{G}_{12}(\omega)$. We first discuss the line broadening resulting only from the nonparabolicity of the conduction band, i.e., we consider behavior of the function $\mathrm{Im}\tilde{G}_{12}(\omega)$ in the limit α_{nn}, $\Gamma\to0$. [Note that when $\alpha_{nn}=0$ then $\tilde{G}_{1n}(\omega)=G_{1n}(\omega)$.] Using the relation $\lim_{a\to0}[a/(x^2+a^2)\pi]=\delta(x)$ and performing the integration in Eq. (6) we find

$$\mathrm{Im}G_{1n}(\omega)=F_{n1}[k_t=k_{n1}(\omega)]\Theta(E_{n1}-\hbar\omega)\times[\mathcal{E}_{n1}^2E_W/(\hbar\omega)^3-\hbar\omega/E_W]\times E_{n1}^2m_W/4\hbar^3\omega N_s\ , \tag{8}$$

where $k_{n1}(\omega)$ is the solution of $E_{n1}(k_t)=\hbar\omega$ and is given by

$$k_{n1}^2(\omega)=[(\hbar\omega/E_W)^2+(\mathcal{E}_{n1}/\hbar\omega)^2-1-2(\mathcal{E}_n+\mathcal{E}_1)/E_W]E_Wm_W/2\hbar^2\ . \tag{9}$$

Here $\Theta(x)$ is the unit step function, $\mathcal{E}_n\equiv\mathcal{E}_{Wl}(k_t=0)$ and $\mathcal{E}_{n1}=\mathcal{E}_n-\mathcal{E}_1$.

Figure 2 presents the variation of $\mathrm{Im}G_{12}$ with ω in the 75-Å GaAs/$Al_{0.35}Ga_{0.65}$As QW for different temperatures and surface carrier concentrations. (In this paper we neglect for simplicity the dependence of the band parameters on T.) We see that at $T\sim0$ function $\mathrm{Im}G_{12}(\omega)$ has nearly rectangular shape. In higher temperatures it becomes strongly asymmetric.

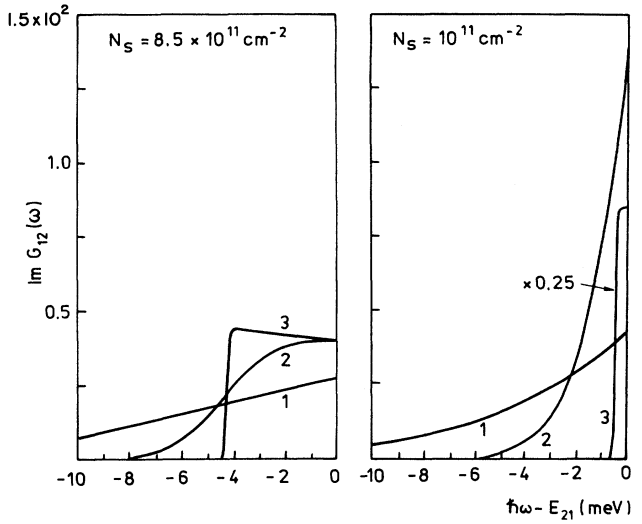

FIG. 2. Calculated imaginary part of $G_{12}(\omega)$ in 75-Å $GaAs/Al_{0.35}Ga_{0.65}As$ QW's with $N_s=1$ and 8.5×10^{11} cm^{-2} at temperatures: (1) $T=300$ K, (2) $T=77$ K, (3) $T=4$ K. $\Gamma=0$.

The variation of the linewidth $\Delta\nu_{12}$ (full width at half maximum) with N_s in QW's with $L=75$ and 100 Å for a couple of temperatures is shown in Fig. 3. We find rather strong dependence of $\Delta\nu_{12}$ on N_s and T. The numerical values of $\Delta\nu_{12}$ are very close to that obtained with the help of the more sophisticated models.[3,4]

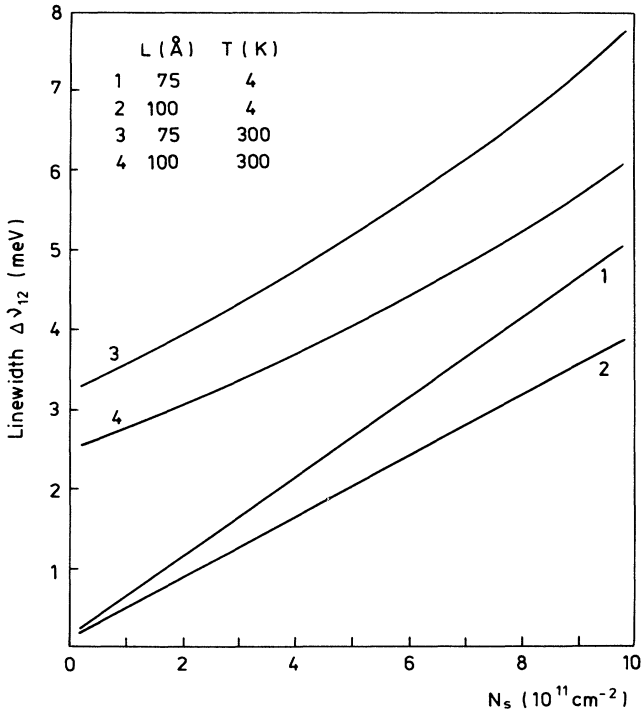

FIG. 3. Linewidth $\Delta\nu_{21}$ vs electron concentration N_s for $GaAs/Al_{0.35}Ga_{0.65}As$ QW's of different thicknesses at various temperatures. $\Gamma=0$.

The room-temperature values of $\Delta\nu_{12}$ (in $GaAs/Al_xGa_{x-1}As$ QW's with $L<100$ Å and $N_s<10^{12}$ cm^{-2}) reported in the literature are in the range 6.5–21 meV.[3,15–18] These values are noticeably larger than that resulting from Fig. 3, which suggests that line broadening induced by collisions is also important. The full line shape arising from nonparabolicity and scattering can be calculated only numerically. We have performed such calculations for a 75-Å GaAs QW (the same as that in Fig. 2) taking $\Gamma=5$ meV. Theoretical absorption line shapes (see Fig. 4) have at low temperature roughly Lorentzian shape. At room temperature our model, as well as those developed in Refs. 3 and 4, predicts a strong asymmetry of the absorption line whereas experimental lines are almost symmetrical.

It is well known that in the case of parabolic subbands [where $E_{n1}(k_t)=E_{n1}(0)$] the resonance screening shifts the peak energy from E_{n1} to $\tilde{E}_{n1}=E_{n1}(1+\alpha_{nn})^{1/2}$ but does not affect the line shape (if we work in the two-subband approximation[14]). We show below that the situation changes drastically when subband separation de-

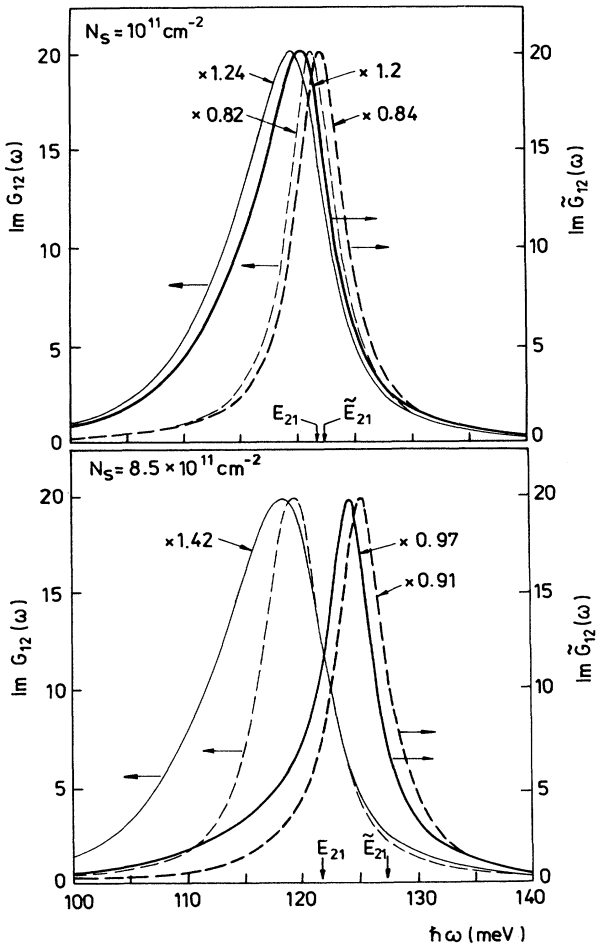

FIG. 4. Calculated imaginary part of $G_{12}(\omega)$, $\tilde{G}_{12}(\omega)$ and the position E_{21} and $\tilde{E}_{21}$ in 75-Å $GaAs/Al_{0.35}Ga_{0.65}As$ QW's with $N_s=1$ and 8.5×10^{11} cm^{-2} at $T=4$ K (dashed lines) and $T=300$ K (solid lines). $\Gamma=5$ meV.

pends on k_t. (In the QW's considered here this dependence arises mainly from the bulk conduction band nonparabolicity.) To calculate numerically the function $\mathrm{Im}\tilde{G}_{1n}(\omega)$, which describes absorption line shape modified by the depolarization effect, we must know the value of L_{nn}. In first approximation, we can estimate L_{nn} using the eigenfunction of the infinite square well potential. This procedure yields the value $(L_{22}/L)=0.056$.[13] (The exact result can be slightly larger due to the tunneling of the envelope function into the $Al_xGa_{1-x}As$ barriers.[13,18])

The shape of the function $\mathrm{Im}\tilde{G}_{12}(\omega)$ for the 75-Å $GaAs/Al_{0.35}Ga_{0.65}As$ QW's is shown in Fig. 4. We find from this figure that the change in line shape induced by resonance screening depends sensitively on the size of α_{22}. In the QW with $N_s=10^{11}$ cm^{-2} factor α_{22} is extremely small ($\alpha_{22}\approx 0.011$) and the modification of the line induced by resonance screening can be practically neglected. However, we must remember that the experiments have been usually performed on the samples with $N_s\approx(5-10)\times 10^{11}$ cm^{-2} ($\alpha_{22}\approx 0.055-0.11$). From Fig. 4 we see that the modification of the line shape is then significant. Note that the depolarization effect not only shifts the peak position to the high energy (by an amount $\Delta_{12}\approx E_{21}[(1+\alpha_{22})^{1/2}-1]$) but also tends to compensate the line distortion induced by different curvature of the subbands. This finding leads us to the conclusion that probably not the mass renormalization due to the electron-electron interaction or polaron effect, as suggested by some authors,[3] but rather the depolarization effect is the main reason why observed in $GaAs/Al_xGa_{x-1}As$ QW spectra have much smaller asymmetry than that resulting from the one-electron theory developed in Refs. 3 and 4. At this point it is interesting also to note that in In-Ga-As/In-Al-As QW's (where the intersubband absorption has recently been also observed[16,18,19]) the asymmetry of the spectrum is more pronounced due to the larger value of γ_W in this system.

The paper was supported by the Ministry of the National Education under Contract No. 2/IF/R.

[1]D. J. Newson and A. Kurobe, Semicond. Sci. Technol. **3**, 786 (1988).
[2]Z. Ikonić, V. Milanović, D. Tjapkin, and S. Pajević, Phys. Rev. B **37**, 3097 (1988).
[3]P. Von Allmen, M. Berz, G. Petrocelli, K. F. Reinhart, and G. Harbeke, Semicond. Sci. Technol. **3**, 1211 (1988); P. Von Allmen, M. Berz, K. F. Reinhart, and G. Harbeke, Superlatt. Microstruct. **5**, 259 (1989).
[4]Z. Ikonić, V. Milanović, and D. Tjapkin, Solid State Commun. **72**, 835 (1989).
[5]G. Bastard, Phys. Rev. B **24**, 5697 (1981); **25**, 7584 (1982).
[6]R. Eppenga, M. F. H. Schuurmans, and S. Colak, Phys. Rev. B **36**, 1554 (1987).
[7]D. L. Smith and C. Mailhiot, Phys. Rev. B **33**, 8345 (1986).
[8]U. Eckenberg, Phys. Rev. B **36**, 6152 (1987).
[9]D. F. Nelson, R. C. Miller, and D. A. Kleinman, Phys. Rev. B **35**, 7770 (1987).
[10]K. H. Yoo, L. R. Ram-Mohan, and D. F. Nelson, Phys. Rev. B **39**, 12 808 (1989).
[11]V. Milanović, Phys. Status Solidi B **136**, 661 (1986).
[12]T. Ando, J. Phys. Soc. Jpn. **44**, 475 (1978).
[13]A. Pinczuk and J. M. Worlock, Surf. Sci. **113**, 69 (1982).
[14]S. J. Allen, Jr., D. C. Tsui, and B. Vinter, Solid State Commun. **20**, 425 (1976).
[15]L. C. West and S. J. Eglash, Appl. Phys. Lett. **46**, 1156 (1985).
[16]B. F. Levine, R. J. Malik, J. Walker, K. K. Choi, C. G. Bethea, D. A. Kleinman, and J. M. Vandenberg, Appl. Phys. Lett. **50**, 273 (1987); K. K. Choi, B. F. Levine, R. J. Malik, J. Walker and C. G. Bethea, Phys. Rev. B **35**, 4172 (1987); B. F. Levine, A. Y. Cho, J. Walker, R. J. Malik, D. A. Kleinman, and D. L. Sivco, Appl. Phys. Lett. **52**, 1481 (1988); B. Levine, C. G. Bethea, K. K. Choi, J. Walker, and R. J. Malik, *ibid.* **53**, 231 (1988).
[17]J. Y. Anderson and G. Landgren, J. Appl. Phys. **64**, 4123 (1988); J. Y. Anderson and U. Westergen, J. Crystal Growth **93**, 307 (1988).
[18]F. Muller, V. Petrova-Koch, M. Zachau, F. Koch, D. Grutzmacher, R. Meyer, H. Jurgensen, and P. Balk, Semicond. Sci. Technol. **3**, 797 (1988).
[19]H. Lobentanzer, W. Konig, W. Stolz, K. Ploog, T. Elsaesser, and R. J. Bauerle, Appl. Phys. Lett. **53**, 571 (1988).